Supplementary Information

Pt_3Sn Nanoparticles Enriched with SnO_2/Pt_3Sn Interface for Highly Efficient Alcohol Electrooxidation

Zichen Wang,[a] Liang Wang,[a] Wangbin Zhu,[a] Tang Zeng,[a] Wei Wu,[a] Zhao Lei,[a] Yangyang Tan,[a] Haifeng Lv,*[b,c] and Niancai Cheng,*[a]

[a] College of Materials Science and Engineering, Fuzhou University, Fuzhou 350108, Fujian, China

[b.] PEM Fuel Cell Catalyst Research And Development Center, Shenzhen, 518057, Guangdong, China.

[C.] Materials Science Division, Argonne National Laboratory, Argonne, IL 60439, United States

*Corresponding author.

E-mail address: niancaicheng@fzu.edu.cn (Niancai Cheng),

lvhaifenganl@gmail.com (H. Lv),

Electrochemical Measurements

The electrochemical measurements were tested on an Autolab electrochemistry station with a standard three-electrode cell. Platinum wire, a glassy carbon electrode coated with catalyst and Ag/AgCl (sat. KCl) were used as a counter electrode, working electrode and reference electrode, respectively. The potentials in this study were converted to reversible hydrogen electrode (RHE). The working electrodes were modified by deposition of 5 uL uniform catalyst ink on a glassy carbon electrode. The uniform catalyst ink synthesized through ultrasonicated mixing 4 mg of catalyst in 1 mL deionized water 20 μL Nafion (5 wt.%) and 1 mL isopropyl alcohol and. Cyclic voltammetry (CV) measurements were carried out in 0.5 M H_2SO_4 at a scan rate of 50 mV s^{-1}. The ethanol oxidation reaction or methanol oxidation reaction was performed in 0.5 M H_2SO_4 + 1 M ethanol or 0.5 M H_2SO_4 + 1 M methanol at a scan of 50 mV s^{-1}. The CO stripping voltammetry was performed in 0.5 M CO-free H_2SO_4 electrolyte at a scan of 50 mV s^{-1} after the electrode was held at 0.05 V vs. RHE in 0.5 M H_2SO_4 solution bubbled with CO for 30 min.

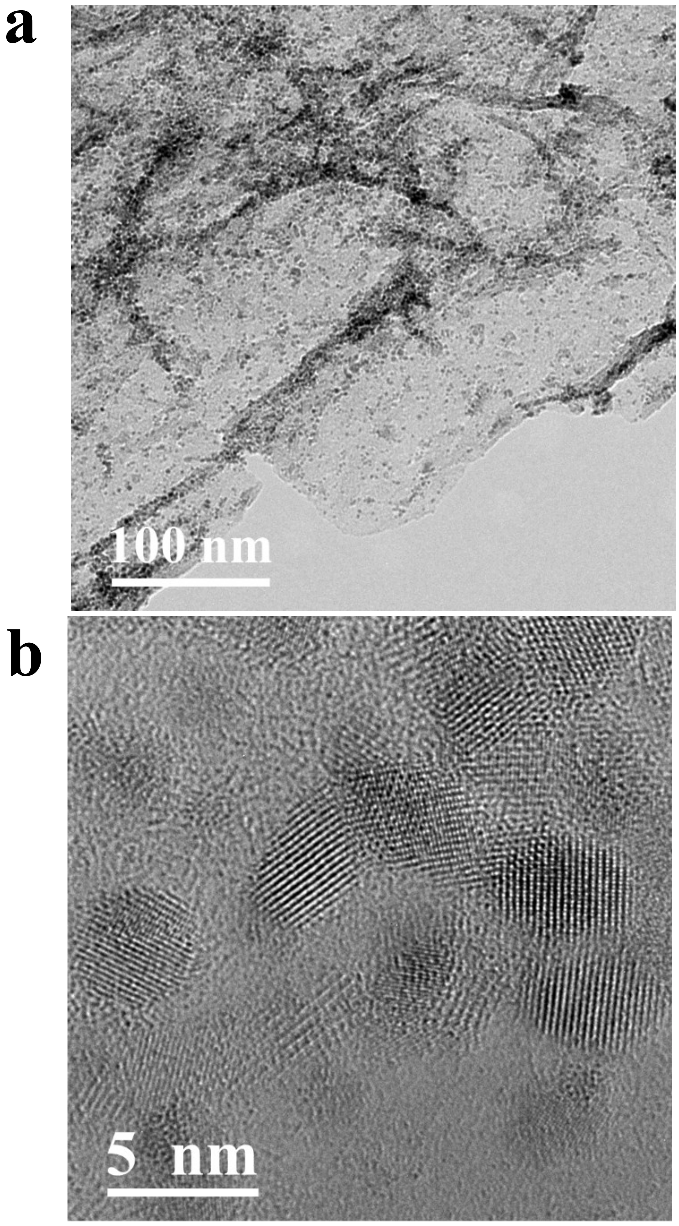

Fig. S1 (a) TEM and (b) HRTEM of Pt_2Sn/NG catalyst.

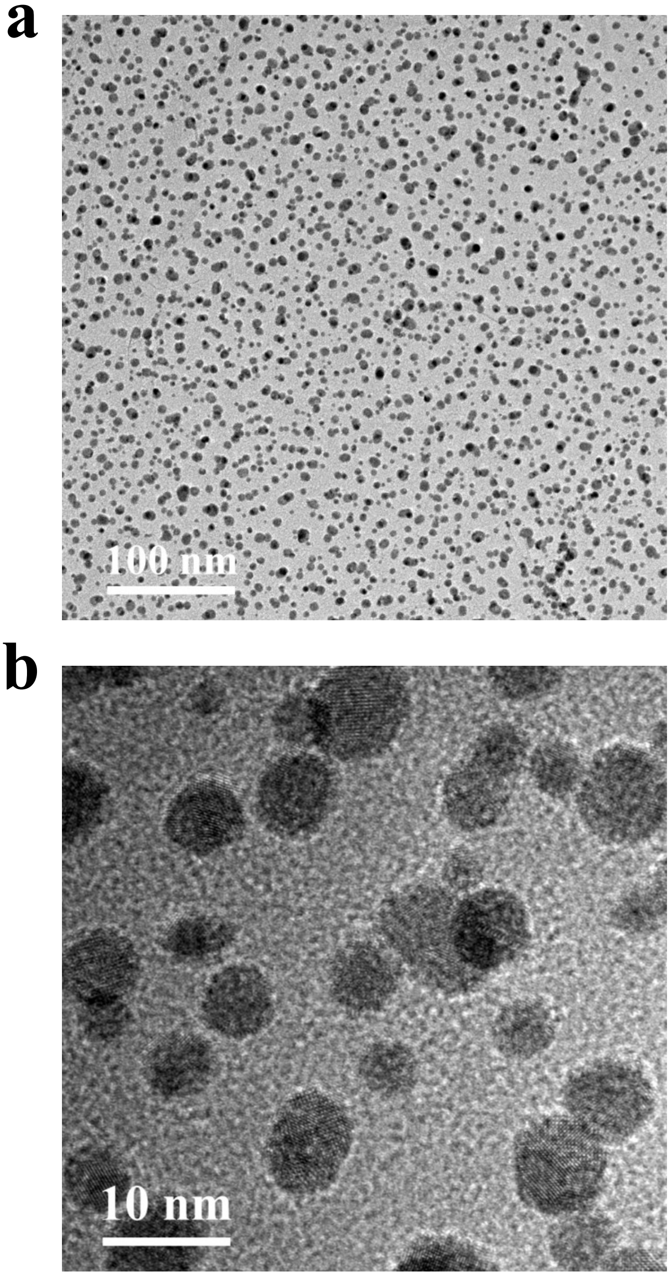

Fig. S2 (a) TEM and (b) HRTEM of Pt_2Sn-H/NG catalyst.

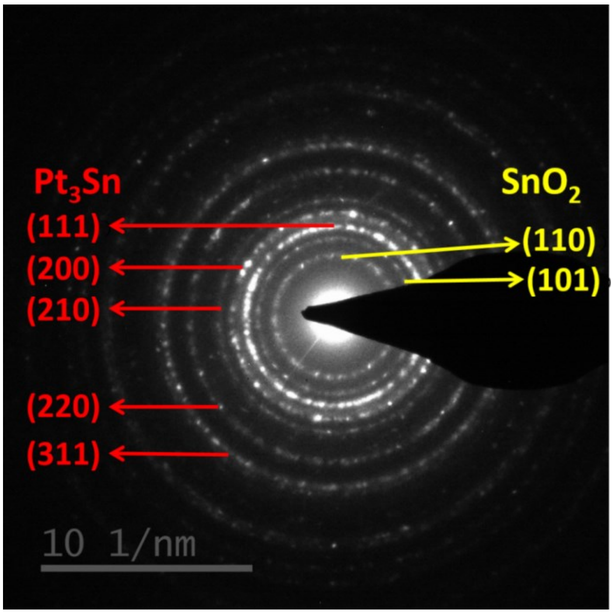

Fig. S3 The selected diffraction pattern of Pt_3Sn@u-SnO_2/NG catalyst.

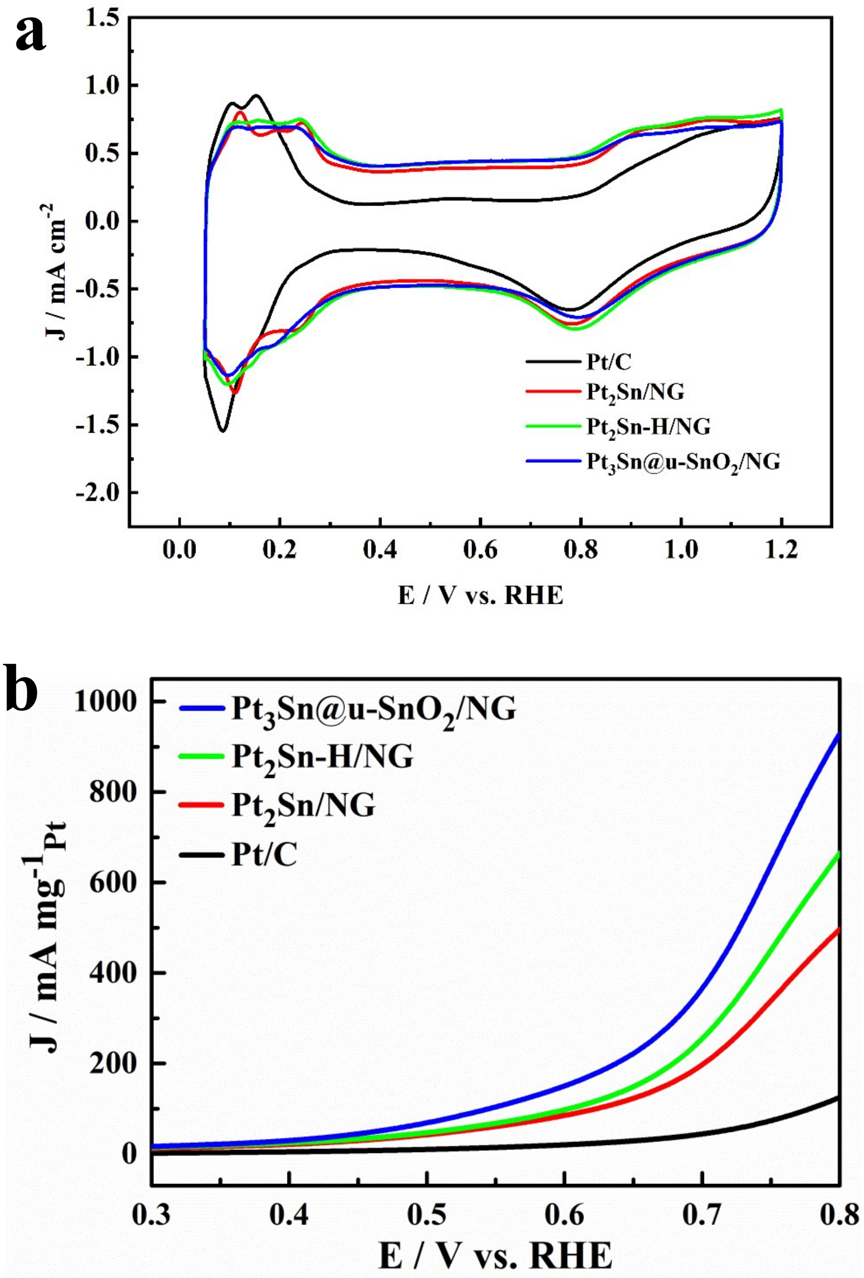

Fig. S4 (a) CV curves of different catalysts in 0.5 M H_2SO_4 solution with a sweep rate of 50 mV s-1. (b) Linear sweep voltammograms of different catalysts in 0.5 M H_2SO_4 + 1 M CH_3CH_2OH solution with a sweep rate of 50 mV s^{-1}.

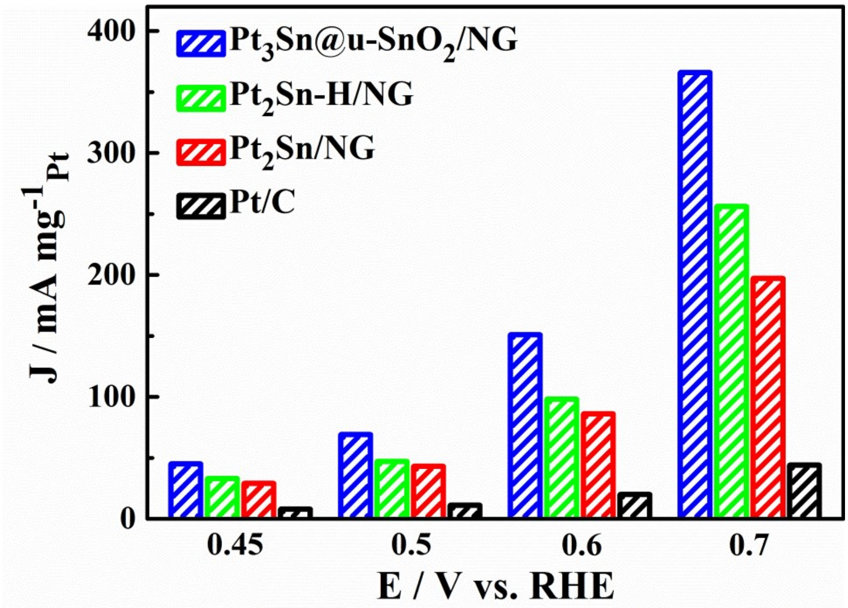

Fig. S5 The mass activity towards EOR on Pt_2Sn/NG, Pt_2Sn-H/NG, Pt_3Sn@u-SnO_2/NG and Pt/C catalysts at different potential.

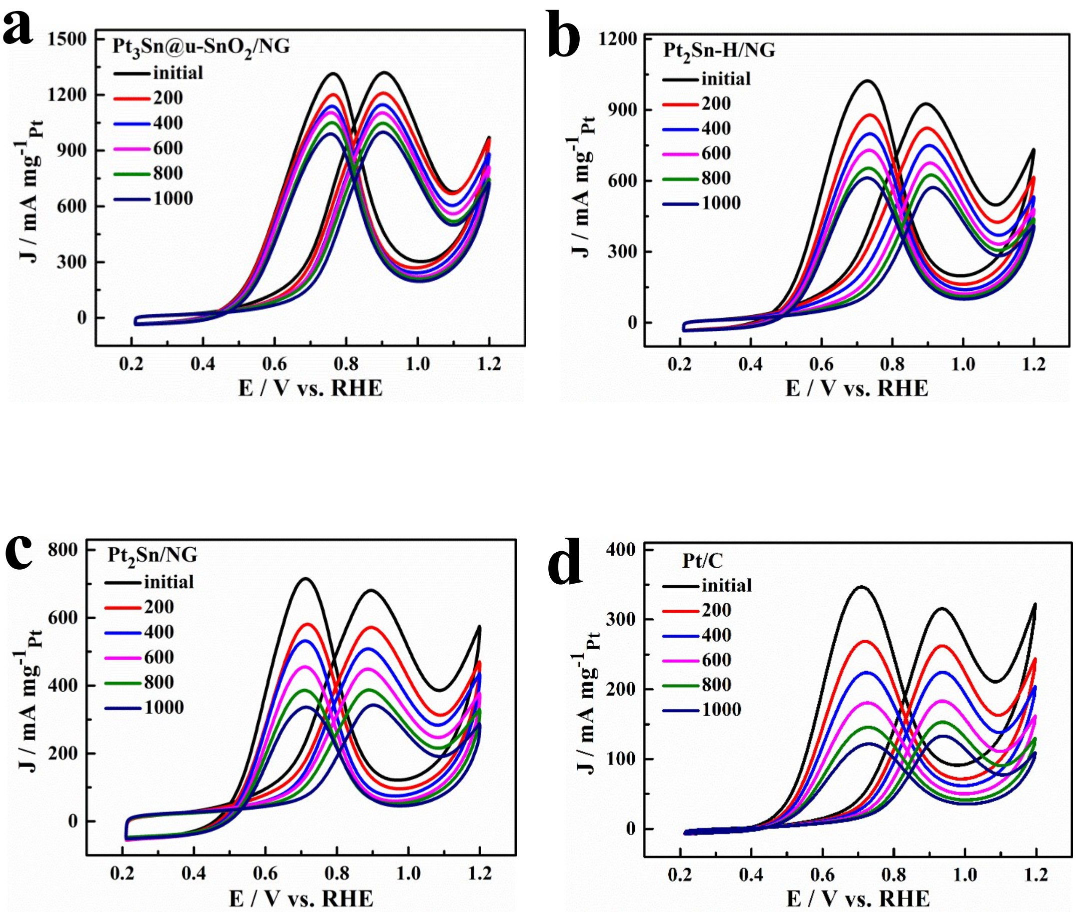

Fig. S6 Cyclic voltammogram of (a) Pt_3Sn@u-SnO_2/NG, (b) Pt_2Sn-H/NG, (c) Pt_2Sn/NG and (d) Pt/C catalysts in N_2-saturated 0.5 M H_2SO_4 + 1 M CH_3CH_2OH solution at scan rate of 50 mV s^{-1} during the durability tests.

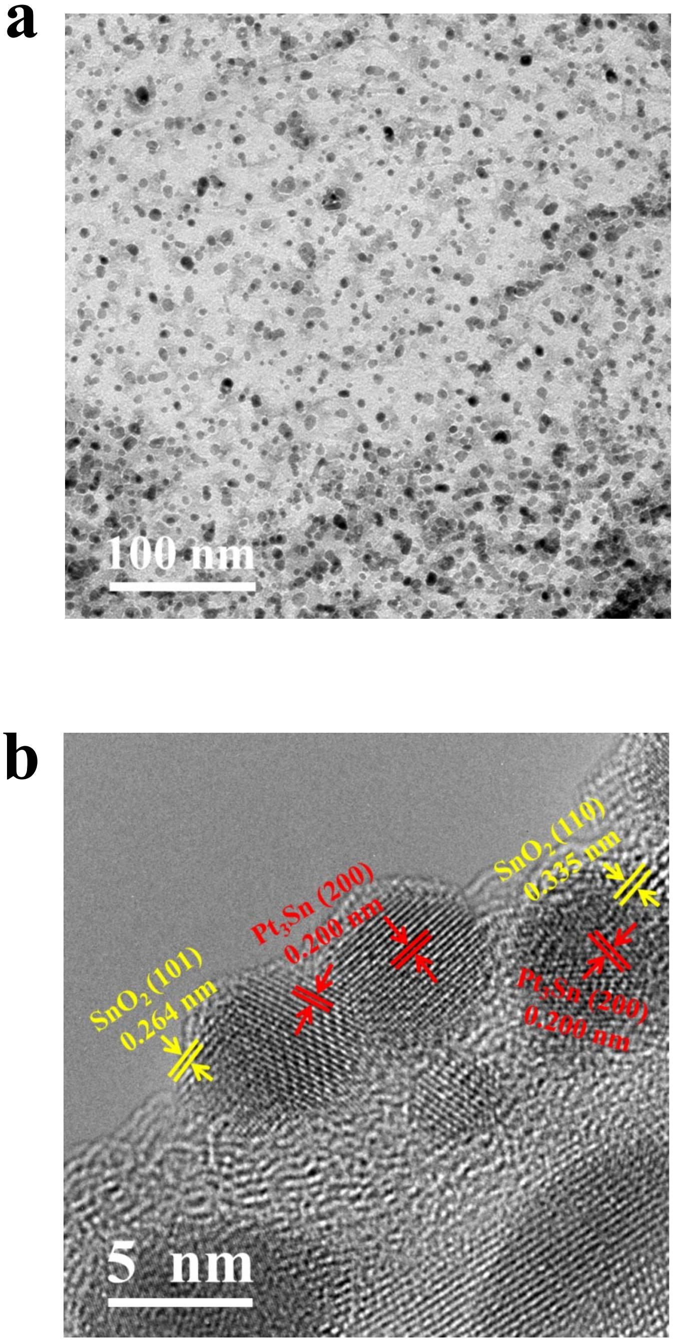

Fig. S7 (a) TEM and (b) HRTEM of Pt_3Sn@u-SnO_2/NG catalyst after the durability tests for 1000 cycles in N_2-saturated 0.5 M H_2SO_4 + 1 M CH_3CH_2OH solution.

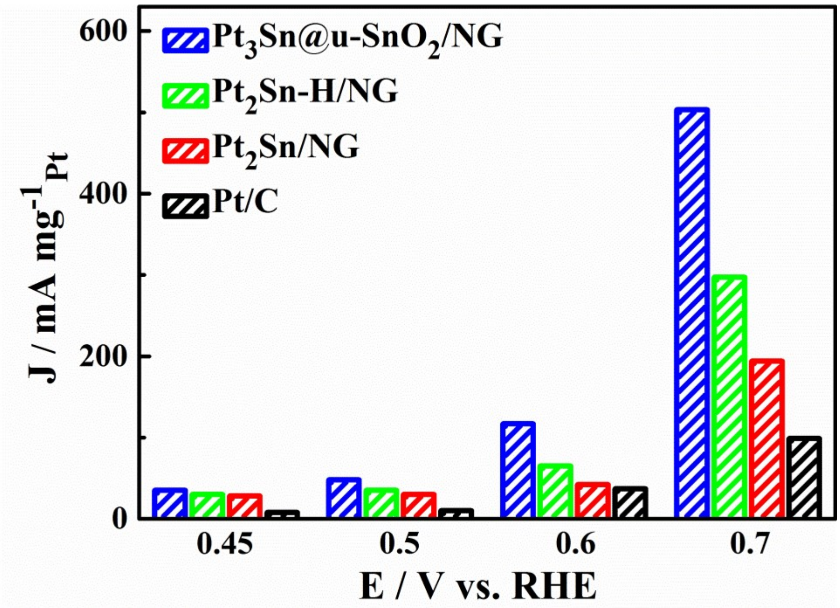

Fig. S8 The mass activity towards MOR on Pt_2Sn/NG, Pt_2Sn-H/NG, Pt_3Sn@u-SnO_2/NG and Pt/C catalysts at different potential.

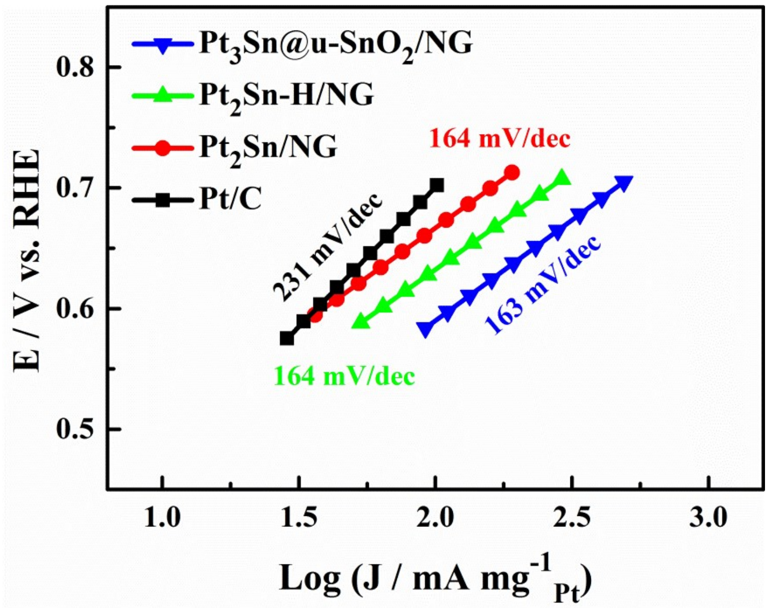

Fig. S9 Corresponding Tafel plots for MOR on Pt_2Sn/NG, Pt_2Sn-H/NG, Pt_3Sn@u-SnO_2/NG and Pt/C catalysts.

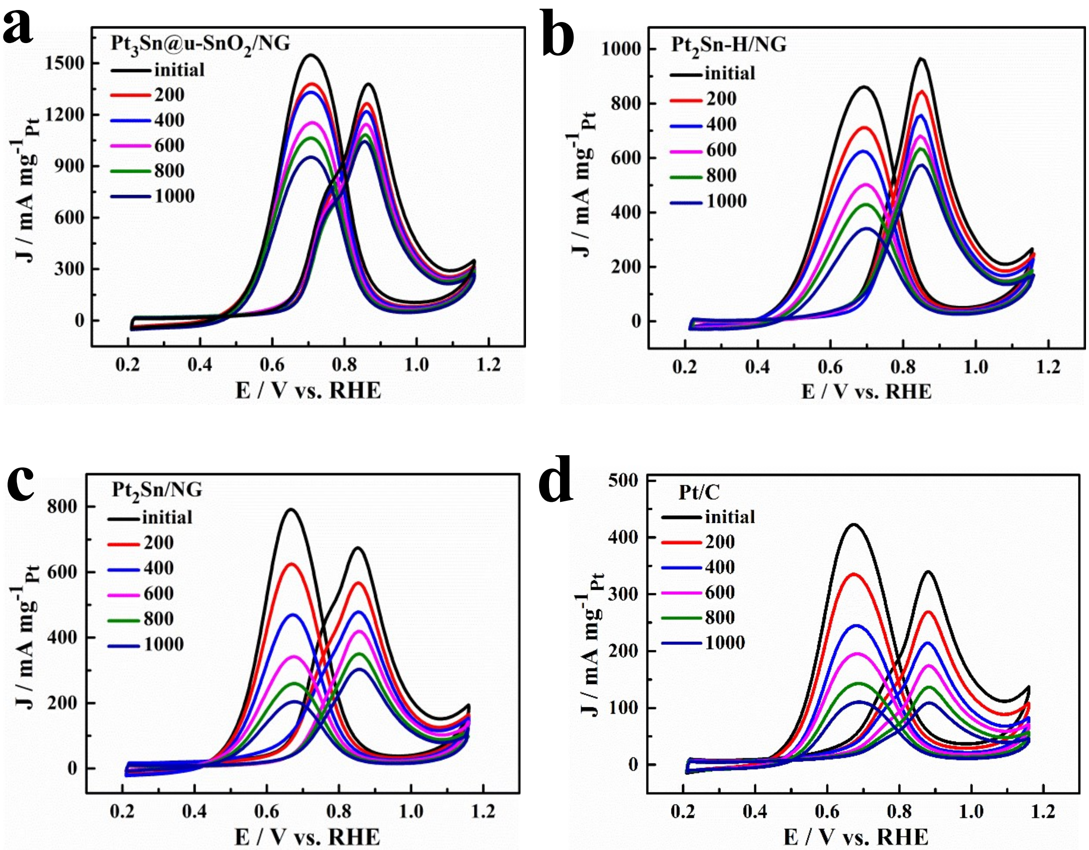

Fig. S10 Cyclic voltammogram of (a) Pt_3Sn@u-SnO_2/NG, (b) Pt_2Sn-H/NG, (c) Pt_2Sn/NG and (d) Pt/C catalysts in N_2-saturated 0.5 M H_2SO_4 + 1 M CH_3OH solution at scan rate of 50 mV s^{-1} during the durability tests.

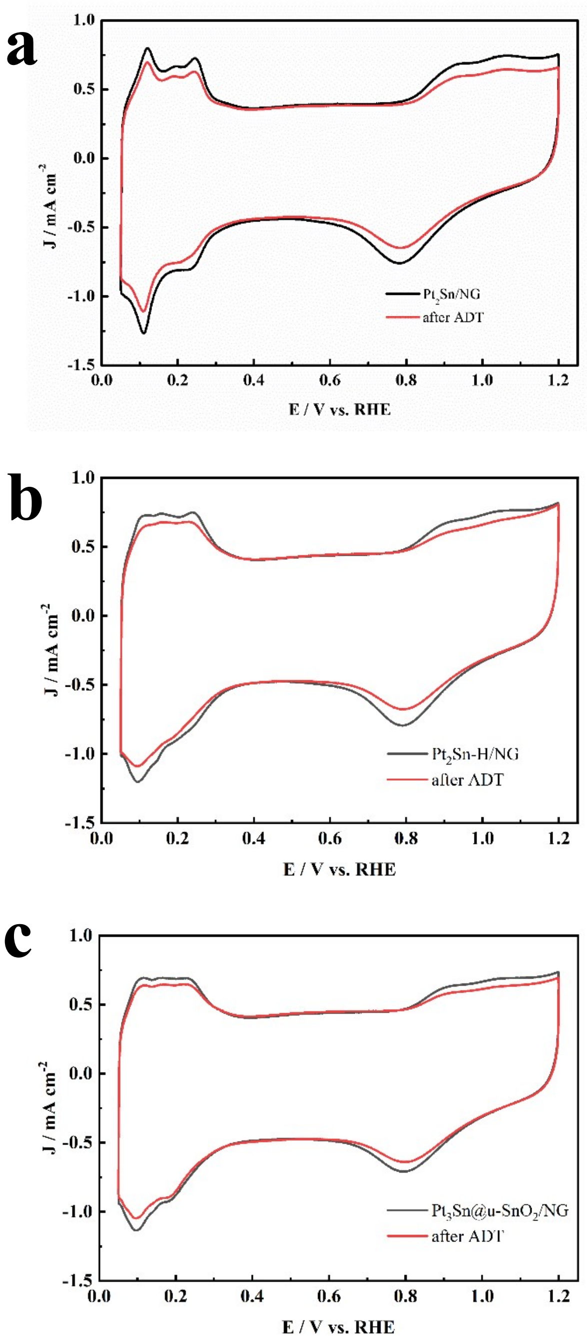

Fig. S11 Cyclic voltammogram of (a) Pt_3Sn@u-SnO_2/NG, (b) Pt_2Sn-H/NG, (c) Pt_2Sn/NG catalysts in N_2-saturated 0.5 M H_2SO_4 solution at scan rate of 50 mV s^{-1} during the durability tests.

Table S1. The peak height ratio of crystal plane.

	(111)	(200)
Standard Pt_3Sn	100	39
Standard Pt	100	53
Pt_3Sn	100	40.6

Table S2. XPS spectra of different catalysts with Pt 4f.

Samples	$Pt^0 4f_{7/2}$	$Pt^{2+} 4f_{7/2}$	$Pt^0 4f_{5/2}$	$Pt^{2+} 4f_{5/2}$
Pt_2Sn/NG	71.49	72.69	74.77	76.08
Pt_2Sn-H/NG	71.23	72.42	74.59	75.77
Pt_3Sn@u-SnO_2/NG	71.32	72.50	74.61	75.90
Pt/C	71.76	72.96	75.10	76.27

Table S3. XPS spectra of different catalysts with Sn 3d.

Samples	$Sn^{4+}3d_{5/2}$	$Sn^{0}3d_{5/2}$	$Sn^{4+}3d_{3/2}$	$Sn^{0}3d_{3/2}$
Pt_2Sn/NG	486.98	485.51	495.41	494.04
Pt_2Sn-H/NG	486.88	485.53	495.34	494.01
Pt_3Sn@u-SnO_2/NG	486.93	485.51	495.34	494.06

Table S4. The valent state mass percent of Sn^0 and Sn^{4+} for different samples.

Samples	Sn^0	Sn^{4+}
Pt_2Sn/NG	2.1	97.9
Pt_2Sn-H/NG	8.5	91.5
Pt_3Sn@u-SnO_2/NG	2.4	97.6

Table S5. EOR Electrochemical activity of the catalysts reported in the literature currently and compared with our $Pt_3Sn@u-SnO_2/NG$ catalyst.

Catalysts	Onset Potential (V vs. RHE) from CO	Peak currents MA ($mA\ mg^{-1}_{Pt}$)	Electrolytes	Ref.
$Pt_3Sn@u-SnO_2/NG$	0.36	1322	0.5 M H_2SO_4 + 1 M CH_3CH_2OH	This work
PtSn	/	764.1	0.5 M H_2SO_4 + 1 M CH_3CH_2OH	[1]
$L1_0$-$Co_{41}Pt_4$ Au_{15}	/	1550	0.1 M $HClO_4$ + 2 M CH_3CH_2OH	[2]
PtRu@FeP	~0.5	660	0.5 M H_2SO_4 + 1 M CH_3CH_2OH	[3]
$Pt_{49}Ru_{51}/C$	/	~630	0.1 M $HClO_4$ + 0.5 M CH_3CH_2OH	[4]
$Pt_3Co@Pt/PC$	/	~830	0.1 M H_2SO_4 + 0.1 M CH_3CH_2OH	[5]
Pt−Ni NFs/C	/	1040	0.1 M $HClO_4$ + 0.2 M CH_3CH_2OH	[6]
PtRu/C	0.75	771	1 M $HClO_4$ + 1 M CH_3CH_2OH	[7]
Pt-$Ce_{0.6}Zr_{0.4}$/C	0.42	272	1 M $HClO_4$ + 1 M CH_3CH_2OH	[7]
Pt_6Sn_3 NWs	/	1080	0.1 M $HClO_4$ + 0.5 M CH_3CH_2OH	[8]
Pt/C + TiO_2	~0.67	648	1 M $HClO_4$ + 1 M CH_3CH_2OH	[9]
Pt/SnO_2/graphene	/	713	0.5 M H_2SO_4 + 0.5 M CH_3CH_2OH	[10]
$SnO_2/Pt/G_{30}$	/	454	0.5 M H_2SO_4 + 0.25 M CH_3CH_2OH	[11]
PZCNT (1:1)	0.52	660	1 M $HClO_4$ + 1 M CH_3CH_2OH	[12]
Pt-CoSn/C	/	~454	0.5 M H_2SO_4 + 0.5 M CH_3CH_2OH	[13]

Table S6. MOR Electrochemical activity of the catalysts reported in the literature currently and compared with our $Pt_3Sn@u\text{-}SnO_2/NG$ catalyst.

Catalysts	Onset Potential (V vs. RHE) from CO	Peak currents MA (mA mg^{-1}_{Pt})	Electrolytes	Ref.
$Pt_3Sn@u\text{-}SnO_2/NG$	0.36	1377	0.5 M H_2SO_4 + 1 M CH_3OH	This work
$Pt_3CoRu/C@NC$	0.35	970	0.1 M $HClO_4$ + 0.5 M CH_3OH	[14]
PtRu@FeP	~0.5	700	0.5 M H_2SO_4 + 1 M CH_3OH	[3]
PZCNT (1:1)	0.52	847	1 M $HClO_4$ + 1 M CH_3OH	[12]
Pt/H-TiO2@N-HPCN-800	0.465	695	0.5 M H_2SO_4 + 1 M CH_3OH	[15]
$Pt_{32}Cu_{68}$ alloy	0.48	707	0.5 M H_2SO_4 + 0.5 M CH_3OH	[16]
$Pt_{3.5}Pb$ NNWs	/	1180	0.5 M H_2SO_4 + 1 M CH_3OH	[17]
Pt–Fe–Mn UCNC	0.43	950	0.5 M H_2SO_4 + 2 M CH_3OH	[18]
Pd@PtNi NPs	~0.65	782	0.5 M H_2SO_4 + 0.5 M CH_3OH	[19]
PtFe@PtRuFe	0.39	690	0.1 M $HClO_4$ + 0.5 M CH_3OH	[20]
Pt/Pd NSLs-WPAS	/	952	0.5 M H_2SO_4 + 0.5 M CH_3OH	[21]
PtRuCu/C	~0.6	1350	0.1 M $HClO_4$ + 1 M CH_3OH	[22]
$Pt_{94}Zn_6$ NWs	~0.65	511.3	0.1 M $HClO_4$ + 0.2 M CH_3OH	[23]
PtRu NWs	/	820	0.1 M $HClO_4$ + 0.5 M CH_3OH	[24]
Pt-CoSn/C	/	970	0.1 M $HClO_4$ + 0.5 M CH_3OH	[25]

References:

[1] Wu, F.; Zhang, D.; Peng, M.; Yu, Z.; Wang, X.; Guo, G.; Sun, Y., *Angewandte Chemie* **2016,** *55*, 4952-6.

[2] Li, J.; Jilani, S. Z.; Lin, H.; Liu, X.; Wei, K.; Jia, Y.; Zhang, P.; Chi, M.; Tong, Y. J.; Xi, Z.; Sun, S., *Angewandte Chemie* **2019,** *58*, 11527-11533.

[3] Bao, Y.; Wang, F.; Gu, X.; Feng, L., *Nanoscale* **2019,** *11*, 18866-18873.

[4] Zhao, Y.; Maswadeh, Y.; Shan, S.; Cronk, H.; Skeete, Z.; Prasai, B.; Luo, J.; Petkov, V.; Zhong, C.-J., *The Journal of Physical Chemistry C* **2017,** *121*, 17077-17087.

[5] Zhang, B.-W.; Sheng, T.; Wang, Y.-X.; Qu, X.-M.; Zhang, J.-M.; Zhang, Z.-C.; Liao, H.-G.; Zhu, F.-C.; Dou, S.-X.; Jiang, Y.-X.; Sun, S.-G., *ACS Catalysis* **2016,** *7*, 892-895.

[6] Ding, J.; Bu, L.; Guo, S.; Zhao, Z.; Zhu, E.; Huang, Y.; Huang, X., *Nano Lett* **2016,** *16*, 2762-7.

[7] Bai, Y.; Wu, J.; Qiu, X.; Xi, J.; Wang, J.; Li, J.; Zhu, W.; Chen, L., *Applied Catalysis B: Environmental* **2007,** *73*, 144-149.

[8] Song, P.; Cui, X.; Shao, Q.; Feng, Y.; Zhu, X.; Huang, X., *Journal of Materials Chemistry A* **2017,** *5*, 24626-24630.

[9] Yu, L.; Xi, J., *Electrochimica Acta* **2012,** *67*, 166-171.

[10] Qu, Y.; Gao, Y.; Wang, L.; Rao, J.; Yin, G., *Chemistry* **2016,** *22*, 193-8.

[11] Qu, Y.; Li, C.; Wang, L.; Gao, Y.; Rao, J.; Yin, G., *International Journal of Hydrogen Energy* **2016,** *41*, 14036-14046.

[12] Song, H.; Qiu, X.; Li, F., *Applied Catalysis A: General* **2009,** *364*, 1-7.

[13] Wang, H.; Zhang, X.; Wang, R.; Ji, S.; Wang, W.; Wang, Q.; Lei, Z., *J. Power Sources* **2011,** *196*, 8000-8003.

[14] Wang, Q.; Chen, S.; Lan, H.; Li, P.; Ping, X.; Ibraheem, S.; Long, D.; Duan, Y.; Wei, Z., *Journal of Materials Chemistry A* **2019,** *7*, 18143-18149.

[15] Zhang, J.; Liu, X.; Xing, A.; Liu, J., *ACS Applied Energy Materials* **2018,** *1*, 2758-2768.

[16] Liao, Y.; Yu, G.; Zhang, Y.; Guo, T.; Chang, F.; Zhong, C.-J., *The Journal of Physical Chemistry C* **2016,** *120*, 10476-10484.

[17] Huang, L.; Han, Y.; Zhang, X.; Fang, Y.; Dong, S., *Nanoscale* **2017,** *9*, 201-207.

[18] Qin, C.; Fan, A.; Zhang, X.; Dai, X.; Sun, H.; Ren, D.; Dong, Z.; Wang, Y.; Luan, C.; Ye, J. Y.; Sun, S. G., *Nanoscale* **2019,** *11*, 9061-9075.

[19] Yu, J.; Li, Q.; Li, Y.; Xu, C.-Y.; Zhen, L.; Dravid, V. P.; Wu, J., *Adv. Funct. Mater.* **2016,** *26*, 7644-7651.

[20] Wang, Q.; Chen, S.; Li, P.; Ibraheem, S.; Li, J.; Deng, J.; Wei, Z., *Applied Catalysis B: Environmental* **2019,** *252*, 120-127.

[21] Xu, G.; Si, R.; Liu, J.; Zhang, L.; Gong, X.; Gao, R.; Liu, B.; Zhang, J., *Journal of Materials Chemistry A* **2018,** *6*, 12759-12767.

[22] Xue, S.; Deng, W.; Yang, F.; Yang, J.; Amiinu, I. S.; He, D.; Tang, H.; Mu, S., *ACS Catalysis* **2018,** *8*, 7578-7584.

[23] Xu, Y.; Cui, X.; Wei, S.; Zhang, Q.; Gu, L.; Meng, F.; Fan, J.; Zheng, W., *Nano Research* **2019,** *12*, 1173-1179.

[24] Huang, L.; Zhang, X.; Wang, Q.; Han, Y.; Fang, Y.; Dong, S., *Journal of the American Chemical Society* **2018,** *140*, 1142-1147.

[25] Huang, L.; Zhang, X. P.; Hang, Y. J.; Wang, Q. Q.; Fang, Y. X.; Dong, S. J., *Chemistry Of Materials* **2017,** *29*, 4557-4562.